Evidence for Fast-Neutron Emission from the Giant Quadrupole Resonance in ^{119}Sn

K. Okada, H. Ejiri, T. Shibata, Y. Nagai, T. Motobayashi, H. Ohsumi, and M. Noumachi
Laboratory of Nuclear Studies and Department of Physics, Osaka University, Osaka 560, Japan

and

A. Shimizu
Research Center for Nuclear Physics, Osaka University, Osaka 565, Japan

and

K. Maeda
College of General Education, Tohoku University, Sendai 980, Japan

(Received 30 November 1981)

Fast-neutron emission from the giant quadrupole resonance in ^{119}Sn was studied for the first time by measuring the deexciting neutrons in coincidence with the inelastic α' from the reaction ^{119}Sn(α, α'). The neutron time-of-flight spectrum shows both the slow evaporation component corresponding to the spreading process and the fast component corresponding to the direct escape leading to single-hole states in the residual nucleus ^{118}Sn.

PACS numbers: 23.90.+w, 24.30.Cz, 25.60.Cy, 27.60.+j

Decay properties of the giant quadrupole resonance (GQR) and other giant resonances (GR) are of current interest in view of the dynamic and microscopic aspects of these resonances. The GR is a kind of collective mode consisting of a coherent sum of one-particle, one-hole (1p-1h) states. Direct particle escape (escape width) from the GR leaves the corresponding one-hole states in the residual nucleus. Successive internucleon collisions (spreading) lead to many-particle, many-hole states, which may eventually deexcite by statistical particle evaporation. Coincidence measurements of deexciting particles with the inelastically scattered particles have recently been carried out to clarify the deexcitation mechanism.[1-16] Most of them have been limited to charged-particle (mostly proton and alpha) decays from the GQR in light and medium-light nuclei.[1-6] Direct decay of the GQR has been observed in ^{16}O [2] and ^{28}Si,[3] while the GQR's of the ^{40}Ca,[4] ^{58}Ni,[5] and Zn isotopes[6] have been suggested to decay by statistical particle emission. Several groups studied the fission process for the GQR in heavy nuclei.[12-16]

The major decay channel of the GQR in medium-heavy nuclei, however, is the neutron decay, because charged particles are greatly suppressed by the Coulomb barrier. If both direct escape and statistical decay coexist in the GQR decay channel of these nuclei, one may observe fast escaping neutrons as well as slow evaporating neutrons. Thus a detailed coincidence measurement of neutrons is crucial to clarify the deexcitation process of the giant resonance in medium-heavy nuclei. One group briefly studied neutrons from the GQR in medium-light nuclei,[5,6] and suggested the statistical decay. Another group recently reported neutron work[8] on the GQR in ^{208}Pb, claiming also the statistical neutron decay.

This Letter reports the first extensive study of fast neutrons from the GQR in medium-heavy nuclei. The nucleus ^{119}Sn was chosen because the low binding energy of neutrons favors observation of the fast neutrons and the high Coulomb barrier greatly inhibits charged-particle emission. The GQR was excited by the inelastic scattering of 109-MeV α particles provided by the Osaka University cyclotron. Measurements were made of energy and angular correlations for the α' particles and the decaying neutrons from the reaction ^{119}Sn$(\alpha, \alpha' n)$. The α' particles were measured by a ΔE-E counter telescope consisting of 8×24-mm$^2 \times 500$-μm position-sensitive silicon surface-barrier (ΔE) and 500-mm$^2 \times 5$-mm Si (E) detectors. It covered the angular range from $\theta_{\alpha'} = 14.6^\circ$ to 23.7°. The neutron energy spectra were measured by a time-of-flight method. Two 5-in.-diam $\times$ 3-in. NE-213 liquid-scintillation counters were set 60 cm apart from the target, one at $\theta_n = -70^\circ$ and another at $\theta_n = 110^\circ$ with respect to the beam. These angles correspond, respectively, to forward and backward angles with respect to the direction of the recoil momentum in the α' scattering.

The GQR with 12.9-MeV excitation energy and 4.2-MeV width is clearly seen as shown in the singles α' spectrum [Fig. 1(a)]. It is in accord with observations for other nuclei.[17] The higher

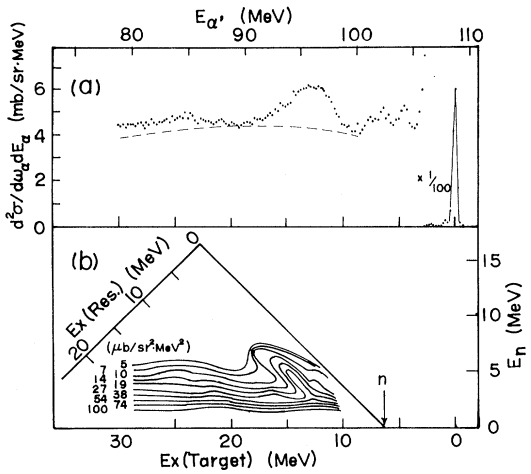

FIG. 1. (a) Singles energy spectrum of the α' particles from the reaction ^{119}Sn(α,α') at $\theta_{\alpha'}=15.8°$. (b) Two-dimensional energy correlation contour map of the α' at $\theta_{\alpha'}=15.8°$ and the decaying neutrons at the recoil backward angle $\theta_n=110°$ for the reaction ^{119}Sn$(\alpha,\alpha' n)$. Equidistant lines of the contour map correspond to an exponential decrease of the cross section with increasing neutron energy E_n for a given excitation energy E_x (target) (namely for given $E_{\alpha'}$).

excitation tail of the GQR at this angle may include some giant monopole component.

Neutrons decaying from the GQR are enhanced at both the recoil forward ($\theta_n=-70°$) and the recoil backward ($\theta_n=110°$) angles. Fast neutrons from the continuum region are due to knockout and preequilibrium processes. In fact, they are emitted preferentially at forward angles with respect to the recoil and the beam axes, and are much reduced at backward angles.[18] Thus observation of the *fast* neutrons from the GQR at the recoil *backward* angle is quite advantageous. The α'-n energy correlation contour map for the reaction ^{119}Sn$(\alpha,\alpha' n)$ observed at the recoil backward angle ($\theta_n=110°$) is shown in Fig. 1(b), where the fast component due to the GQR is significantly enhanced as indicated by the clear bump. This is in contrast to the simple exponential falloff of the yield as E_n increases in the continuum region beyond the GQR excitation energy. The fast-neutron emission from the GQR leaves the residual nucleus ^{118}Sn with excitation energy around 2–4 MeV. This is seen by projecting the bump observed at the GQR excitation region ($E_x=12$–18 MeV) onto the E_x(^{118}Sn) excitation energy axis [see Fig. 1(b)].

The singles α' energy spectra for the angular range from $\theta_{\alpha'}=14.6°$ to 23.7° and the corresponding α' energy spectra gated by the 4–6-MeV fast neutrons are shown in Figs. 2(a) and 2(b), respectively. (Note that the recoil angle

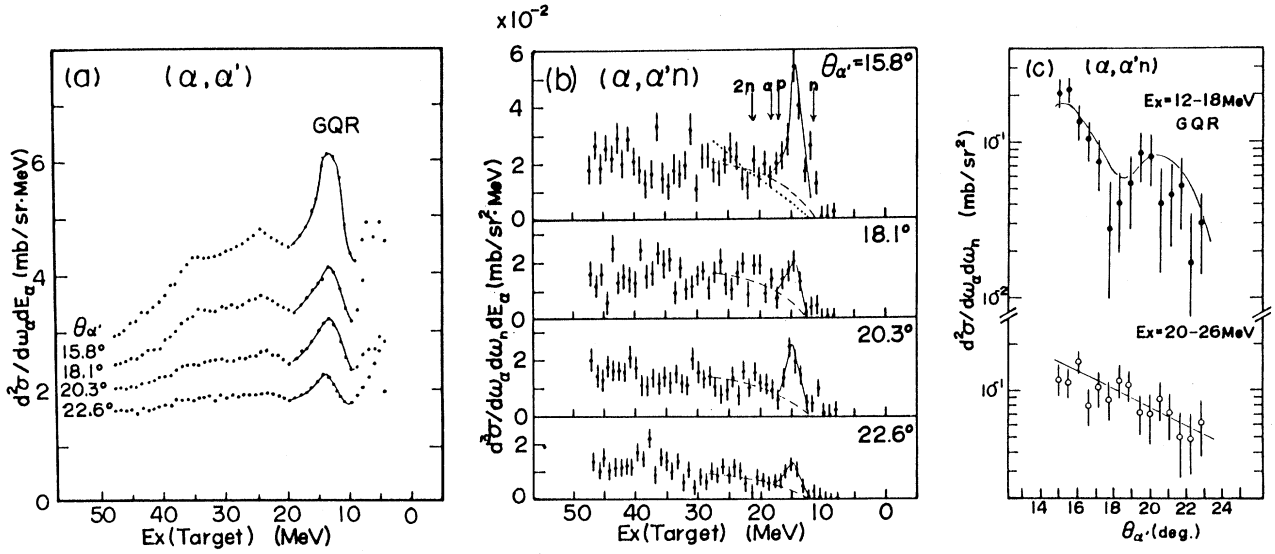

FIG. 2. (a) Singles α' spectra for the reaction ^{119}Sn(α,α'). Each shows the summed spectra over the angular range of $\Delta\theta_{\alpha'}=2.3°$. (b) Coincidence α' spectra gated by 4–6-MeV neutrons at $\theta_n=110°$; $\Delta\theta_{\alpha'}=2.3°$. The dotted line is the Hauser-Feshbach statistical calculation. The arrows indicate the effective separation energies for neutron, proton, alpha, and two-neutron decay channels. Here the neutron kinetic energy of 5 MeV for one neutron and the Coulomb barrier for the charged particles have been corrected for. (c) The angular distributions of (top) the α' bump of the GQR region ($E_x=12$–18 MeV), after subtraction of the background, and (bottom) the continuum region ($E_x=20$–26 MeV) measured in coincidence with the 4–6-MeV fast neutrons at $\theta_n=110°$; $\Delta\theta_{\alpha'}=0.57°$. The solid lines indicate the corresponding angular distributions of the singles spectra.

does not change more than $\Delta\theta_R = 2^\circ$ in the range of the α' detection angle.) The coincidence measurement with the fast neutrons at the recoil backward angle makes the GQR stand out against the underlying continuum background. The emission of the 4–6-MeV gating neutrons costs 11.5 MeV of the separation energy, which is the (γ, n) threshold energy for 4–6-MeV neutron emission from ^{119}Sn. Furthermore, the fast-neutron emission from the GQR of the ^{119}Sn predominantly leaves the 2–4-MeV excited states of ^{118}Sn as shown later. Thus the effective separation energy for such fast neutrons amounts to even 13.5 MeV. Consequently the lower excitation region (12–13 MeV) of the GQR peak is "shaved off" in the n-gated α' spectra [Fig. 2(b)]. This gives rise to a shift of the excitation energy of the GQR peak in the n-gated coincidence spectra [Fig. 2(b)] by 1–2 MeV above the GQR peak energy in the singles spectrum [Fig. 2(a)]. (Actually, the GQR in the α' energy spectrum gated by slow neutrons peaks at the same excitation energy as the GQR in the singles spectrum.)

The present fast neutrons from the GQR are due to the first-stage doorway process, where a fast particle is emitted directly from the GQR consisting of 1p-1h components before statistical equilibration. The cross section of this direct-escape $(\alpha, \alpha' n)$ process is of the order of 0.1 mb/sr^2 MeV at the GQR peak [see Fig. 2(b)]. Evaporation neutrons (mostly below 2 MeV) following the statistical decay hardly contribute to the present α' spectra gated by the 4–6-MeV fast neutrons. Actually, Hauser-Feshbach (HF) calculations including all open channels of p, α, and $2n$ decays do not reproduce the observed GQR peak, as shown in Fig. 2(b). The opening of the proton decay channel effectively around 17 MeV, which is beyond the GQR, has little effect, and the HF calculation gives an extremely small cross section of about 0.0001 mb/sr^2 MeV for the $(\alpha, \alpha' p)$ process around $E_x = 20$ MeV. This is because of the large Coulomb barrier and the large proton separation energy. The opening of the $2n$ decay channel gives only additional slow neutrons, and results in little additional contribution to the present α' spectra gated by the fast neutrons.

The angular distribution of the GQR peaks in the α' spectra gated by the 4–6-MeV neutrons is fitted well by that of the GQR peak in the singles α' spectra [see Fig. 2(c), top]. Here the smooth background has been corrected for [the dashed lines in Fig. 2(b)]. These GQR angular distributions are characteristic of the quadrupole excitation. They are in contrast to the monotonic distributions [Fig. 2(c), bottom] for both the singles and the coincidence α' in the 20–26-MeV continuum region beyond the GQR excitation energy.

The α'-n coincidence measurement in the intervals $\theta_n = -34^\circ$ to -130° and $\theta_n = 40^\circ$ to 130° gave a branching ratio of the order of 20% for the fast escaping neutrons from the GQR. It is much larger than the HF calculation.

The neutron energy spectrum at $\theta_n = 110^\circ$ in coincidence with the α' particles leading to the higher excitation region of the GQR ($E_x = 14.4$ MeV) is shown in Fig. 3(a). This excitation region lies well above the (γ, n) threshold energy, and the directly escaping neutron can have energy large enough to be separated from the evaporating slow neutron. Figure 3(a) gives the population strength of the excited levels in the residual ^{118}Sn after the neutron decay from the GQR and the underlying continuum. The spectrum consists of the slow component with the evaporation pattern and the fast component peaking at $E_n = 4$–6

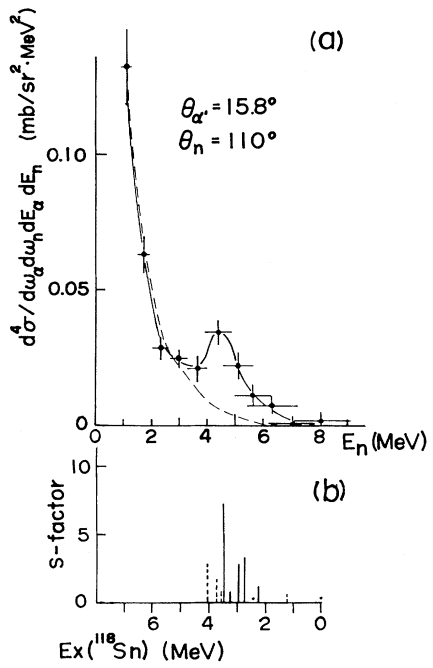

FIG. 3. (a) Energy spectrum of neutrons for the reaction ^{119}Sn$(\alpha, \alpha' n)$ gated by the α' feeding the higher excitation region of the GQR ($E_x = 14.4$ MeV). The dashed line shows the energy spectrum of neutrons decaying from the continuum region of $E_x = 20$ MeV. (b) The spectroscopic factors of the neutron single-hole states in ^{118}Sn obtained by the (p, d) reaction (Ref. 19). Solid, dashed, and dotted lines present $l_n = 4$, 2, and 0 transfers, respectively.

MeV. The slow component agrees, as shown in Fig. 3(a), with the energy spectrum of the neutrons decaying from the non-GQR continuum region with 20 MeV excitation energy, where no strong giant resonances are excited in the present (α, α') reaction. The fast component corresponds to the population of the excited levels around 3.5 MeV in ^{118}Sn. Direct escape of the unbound neutron particle out of the GQR leads to such one-hole states as $(1g_{7/2})^{-1}$, $(2d_{5/2})^{-1}$, $(2d_{3/2})^{-1}$, and $(3s_{1/2})^{-1}$ in ^{118}Sn. The population strength for the fast neutrons following the GQR in ^{119}Sn is in accord with the spectroscopic strength distribution for the single-hole states populated by the reaction ^{119}Sn$(p, d)^{118}$Sn,[19] as shown in Fig. 3(b).

In short, the present $(\alpha, \alpha' n)$ coincidence work demonstrates that the GQR in a medium-heavy nucleus shows up selectively above the continuum by measurement of inelastically scattered particles in coincidence with decaying fast neutrons at backward angles with respect to the recoil axis. Although the fast-neutron branch is a small fraction of the major nondirect spreading process, such direct-escape neutrons carry indeed a microscopic particle-hole feature of the GQR.

The authors thank Professor S. Yoshida for valuable discussions, Dr. M. Sasao and Dr. H. Sakai for kind collaboration, and the Research Center for Nuclear Physics for the beam time assignment with the program number 11A05.

[1]H. Riedesel *et al.*, Phys. Rev. Lett. 41, 377 (1978).
[2]K. T. Knöpfle *et al.*, Phys. Lett. 74B, 191 (1978).
[3]K. T. Knöpfle *et al.*, Phys. Rev. Lett. 46, 1372 (1981).
[4]D. H. Youngblood *et al.*, Phys. Rev. C 15, 246 (1977).
[5]M. T. Collins *et al.*, Phys. Rev. Lett. 42, 1440 (1979).
[6]M. T. Collins, C. C. Chang, and S. L. Tabor, Phys. Rev. C 24, 387 (1981).
[7]W. Eyrich *et al.*, Phys. Rev. Lett. 43, 1369 (1979).
[8]H. Steuer *et al.*, Phys. Rev. Lett. 47, 1702 (1981).
[9]K. T. Knöpfle, in *Nuclear Physics with Electromagnetic Interactions*, edited by H. Arenhövel and D. Drechsel, Lecture Notes in Physics Vol. 108 (Springer, Berlin, 1979), p. 311.
[10]G. J. Wagner, in *Proceedings of the Giant Multipole Resonance Topical Conference*, edited by F. E. Bertrand (Academic, New York, 1980), p. 251.
[11]L. S. Cardman, Nucl. Phys. A354, 173 (1981).
[12]J. van der Plicht *et al.*, Nucl. Phys. A346, 349 (1980).
[13]A. C. Shotter *et al.*, Phys. Rev. Lett. 43, 569 (1979).
[14]J. D. T. Arruda Neto and B. L. Berman, Nucl. Phys. A349, 483 (1980).
[15]F. E. Bertrand *et al.*, Phys. Lett. 99B, 213 (1981).
[16]H. Ströher *et al.*, Phys. Rev. Lett. 47, 318 (1981).
[17]F. E. Bertrand, Nucl. Phys. A354, 129 (1981).
[18]K. Okada *et al.*, in *Proceedings of the International Symposium on Highly Excited States in Nuclear Reaction*, edited by H. Ikegami and M. Muraoka (Osaka University, Osaka, 1980), p. 477; H. Ejiri, in Proceedings of the Seminar on High Energy Nuclear Interactions in Dense Nuclear Matter, Hakone, Japan, 1980 (unpublished), paper No. I-411.
[19]K. Yagi *et al.*, J. Phys. Soc. Jpn. 24, 1167 (1968).

Revised Formulation of the Phenomenological Interacting Boson Approximation

D. D. Warner and R. F. Casten
Brookhaven National Laboratory, Upton, New York 11973
(Received 11 February 1982)

Previous interacting-boson-approximation studies of deformed nuclei have used different forms of the quadrupole operator in the Hamiltonian and $E2$ operators. A revised formalism is proposed which employs consistent operators and embodies a simpler Hamiltonian. It yields improved agreement with the data for deformed nuclei, a number of parameter-free predictions for transition regions, a specific form of the O(6) limit which agrees with that found empirically, and a closer relation to the neutron-proton version of the model, IBA-2.

PACS numbers: 21.60.Fw, 21.60.Ev, 23.20.Lv

The interacting boson approximation[1] (IBA) represents a significant step forward in our understanding of nuclear structure. It offers a simple Hamiltonian, capable of describing collective nuclear properties across a wide range of nuclei, and is founded on rather general algebraic group-theoretical techniques which have also found recent application to problems in atomic, molecular, and high-energy physics.[2,3] The application of the phenomenological version of this model (IBA-1) to deformed nuclei is currently a subject of considerable interest and controversy.[4] Recent

